CONTACT FATIGUE DESIGN OF HELICAL GEAR BY SPUR GEAR EQUIVALENCY

Edward. E. Osakue[1], Lucky Anetor[2]

[1]*Department of Industrial Technology, Texas Southern University, Houston, Texas, USA*
[2]*Department of Mechanical Engineering, Nigerian Defence Academy, Kaduna, Nigeria*

Abstract

Contact fatigue failure or pitting is a common mode of gear failure. High speed gearing is therefore prone to pitting and scoring failure modes. A simplified contact stress capacity model that is explicit in the representation of helical gear design parameters is developed. The model gives estimate of the contact stress expected in a helical gearset during meshing. Also, the model clearly reveals the direct influence of the base helix angle on contact stress and normal module size estimates. Contact stresses for five design Examples from different references are computed using the new contact stress capacity model and compared with AGMA estimates. The results show very favorable comparisons because the percentage variances between the new model and AGMA contact stress estimates are within -10% to 6% in this study. The Examples cover a wide range of the helix angles which spans 15^o to 41.41^o and different normal pressure angles of 20^o and 25^o. The new model appears to give slightly higher contact stress values in general so that for preliminary design, it offers the advantage of providing conservative solutions. The new contact stress capacity model was modified for design sizing and its application is demonstrated in Example 6. Comparison of the service load factor values for design sizing and design verification indicates a difference of only 0.9% in Example 6. The new model may be used for contact fatigue design of spur gears if the helix angle is taken as zero degree.

Keywords: *Hertz Contact Stress, Contact Fatigue Strength, Helix Angle, Base Helix Angle, Service Load Factor*

----------***----------

1. INTRODUCTION

A helical gear has teeth helically wrapped like a thread on its pitch cylinder though the pitch surfaces are cylindrical as in spur gears [1]. The helix may be right-handed or left-handed and its inclination to the axial direction of the gear is called the helix angle. A spur gear may be treated as a helical gear with a zero helix angle [2]. Helical gears can be used to transmit torque and rotational motion between parallel and non-parallel shafts, though the former is more common than the later. The initial contact in helical gear mesh is a point which develops into a diagonal line on the tooth face as the teeth come into more engagement. This leads to a more gradual engagement of meshing teeth and as such a smoother transfer of load from the driving teeth to the driven teeth. Therefore helical gears have the ability to transmit heavy loads at high speeds [3] and run quieter and with less vibration compared to spur gears. They accommodate small variations in center distance and pitch velocity can be over 50 m/s. Due to the helix angle, helical gears exert axial load on supporting shafts in addition to the tangential and radial loads experienced by spur gears.

Helical gears may be classified as narrow-face and wide-face based on their face width. Narrow-face helical gears have face width of at most one axial pitch and are also called low contact ratio (LCR) gears. They have a small face width or low helix angle or both and no facial overlap of gear teeth occurs during transmission. Narrow-face helical gears tend to have a noise level not too different from that of spur gears [3]. Wide-face helical gears have a face width more than one axial pitch and are also called conventional helical gears. When in mesh, they make contacts on two perpendicular planes called transverse and axial, respectively, please refer to Fig. 2. This greatly enhances the chance of more than one pair of teeth being in contact during transmission so that load shearing is higher. Consequently, they have higher load capacity than spur and narrow-face helical gears. Wide-face helical gears are the popular type of helical gears and form the focus of this study.

Narrow-face and wide-face helical gears may be divided into single-helix, double-helix and crossed-helical gears. Single-helix gears have a single right-handed or left-handed helix angle. The most common single-helix gearset is one with opposing helix hands of the gears in mesh and they connect parallel shafts. When two or more single helix-gears are mounted on the same shaft, the hands of the helix angle on the gears should be selected so as to minimize the axial thrust load on the shaft [3]. Double-helix gears have two opposing helices on the same gear blank. Two kinds of double-helix gears are in use and they are herringbone and twain-helical gears. Herringbone gears consist of two helical gears of opposing helix hands on one gear blank without a gap between them. Twain-helical gears consist of two helical gears of opposing helix hands on one gear blank with a gap between them. Thrust loads are practically eliminated in double-helix gears because of the opposing hands of the helix angles on the two faces of the gear. They develop opposite thrust reactions that tend to cancel the axial load components [3]. Double-helix gears are used when high power must be transmitted such as in ship and turbine drives. But they are more expensive compared to single-helix gears. Also they must be precisely located axially to ensure balancing of thrust

loads. Crossed helical gears are helical gear mounted on non-parallel shafts. In mesh, their teeth slide without rolling and are in point contact theoretically, which is different from the line contact of other helical and spur gears [4]. For this reason, crossed helical gears are limited in their load-carrying capacity and as such, are not recommended for use where large torque or power must be transmitted [4]. Partridge [5] has enumerated to some degree, the advantages and disadvantages of single-helix and double-helix gears. To maintain contact across the entire tooth face, the minimum face width of a helical gear must be greater than the axial pitch [6]. Hence a minimum face width of 1.15 or 1.2 times the axial pitch is commonly suggested [1, 3, 4, 6]. Though a face width more than one axial pitch allows more than one tooth pair to be in contact simultaneously in the axial plane, the full benefit of helical tooth action requires a face width of at least two axial pitches [7]. This is beneficial for smooth and quiet running of helical gearsets. Gear design problems become increasingly more complex when complicated tooth shapes are involved [4].

The helix angle has the save value for the pinion and the gear in a helical gearset. For parallel shaft assembly, the hand of the helix angle is opposite on the meshing gears but can be the same for non-parallel shafts. The range of the helix angle is between 5^o to 50^o [5, 6]. Helix angles of 5^o to 25^o are generally used in single-helix gears so as to keep thrust load relatively small [5, 8, 9]. For single-helix gears, the helix angle should not exceed 30^o to avoid excessive axial thrust and it should not be less than 8^o because the advantages of helical gearing become marginal at low helix angles [8]. The helix angle for double-helix gears is generally between 20^o to 45^o [5, 9]. A helix angle of at least 30^o is recommended but a value of about 35^o is preferred [3, 7]. At such values, axial movement from couplings can be resisted. The design of double-helix gears is the same as that of single-helix gears after the transmitted power is halved [9]. It is desirable to have whole number helix angle because it simplifies machine setup for cutting and finishing helical gears [8], thereby reducing manufacturing costs.

Several potential failure modes in gearing have been identified [8, 10], but the two prominent modes are surface fatigue or pitting and bending fatigue [2, 11, 12]. In this study, we are concerned with pitting. Pitting is the appearance of tiny pits on gear tooth surface due to particle detachment because of repeated high contact stress. It has been observed that pitting mostly occurs in the vicinity of the pitch line [8, 13]. Prolong operation after pitting begins roughen the gear tooth surface, resulting in deterioration of form [14]. In a speed reducer drive, the pinion is more vulnerable to pitting because it makes more revolutions per unit time. In a speed increaser drive, the gear is more vulnerable to pitting. At increased pitch point speed, the prospects for pitting and scoring failure modes in gears increase. Tooth failure due to fracture or breakage is rare in double-helix gears. Rather, failure is usually associated with excessive wear or sub-surface gear tooth failures such as pitting and spalling [15]. Pressure above the yield strength of gear materials generally leads to rapid wear.

Pitting occurs in gears when the surface durability of the meshing flanks is exceeded, resulting in crack growth followed by particle break out from the flank [12]. The surface stresses in gear teeth were first investigated in a systematic way by Buckingham [4]. He supposed that the contact of gear teeth can be simulated by two equivalent cylinders in rolling motion. The radii of the equivalent cylinders are obtained by projecting the pitch radii of the gears on the line of action during meshing with contact occurring at the pitch point. The German physicist, Henry Hertz developed expressions for the stresses created when curved frictionless surfaces are loaded in contact in 1881. Thus contact stresses are generally called Hertz stresses and his solution is the basis of pitting failure in gear design. Using Hertz contact stress expressions for two frictionless cylinders in contact, Buckingham developed an equation for gear pitting resistance which has been adopted and modified by national and international standard organizations such as American Gear Manufacturers Association (AGMA) and International Standardization Organization (ISO) in gear design technology. It is believed that a shear stress initiated crack beneath the surface due to excessive repeated Hertz contact stresses gradually develops to the tooth surface and causes shearing away of some materials thus leaving a pit behind. Pitting failure therefore manifests as wear on the flanks and faces of gears and is usually a gradual form of failure. In addition to contact stress, pitting is influenced by sliding velocity, lubricant viscosity, and friction [8].

Pitting can be prevented by keeping contact stresses below the contact fatigue strength. For maximum durability, it is desirable to distribute the wear uniformly amongst all gear teeth. The best case would be that a re-meshing of a pinion tooth occurs after it makes a number of revolutions equal to the number of pinion teeth. This can be achieved by providing a *hunting tooth*. A hunting tooth ensures that the number of teeth on the pinion and gear do not have a common divisor. This means an integer velocity ratio has to be avoided in a gearset transmission. This may be permissible in power transmission gearing where some speed variation can be tolerated. A hunting tooth is undesirable in control gears where precise motion transmission is a main design objective.

Most gears are made of steel of different types such low-carbon, low-alloy, high-carbon, and high-alloy steel materials which may be given different kinds of heat treatments such as normalization, quenched-tempering, and case-hardening. Normalized steel gears come approximately in the hardness range of 160 HVN to 300 HVN, quenched-tempered (Q & T) steel gears come in the hardness range of 300 HVN to 450 HVN and case-hardened steel gears can have surface hardness in the range of 450 HVN to 1000 HVN. Please refer to the Appendix for very brief discussions on steel gear material manufacturing qualities, gear tooth quality numbers and gear assembly classes. Thru-hardened (normalized and quenched-tempered) steel gears are generally more compliant and tolerate to operational errors than case-hardened gears and they tend to generate more noise when gear failure is impending [5]. Very high kilowatt power drives in many

cases require very hard or case-hardened gears so as to keep operating pitch point velocity within allowable limits. However, very hard gears are prone to scoring due to operational high load intensity and sliding velocities [5]. Gear tooth form accuracy for high speed gearing has to be very good in order to minimize internally generated dynamic loads [16].

Helical gears are increasingly being used because of their relatively smooth and quiet operation, large load carrying capacity, and higher operating speed [5, 17]. Single-helix and double-helix gears are mainly used for high speed gearing in parallel shaft connection. Other types of gears are seldom used for high speed applications. Single-helix gears can be used for pitch point speed of up to 50 m/s while double-helix gears may have up to 150 m/s or 200 m/s pitch point speed [6, 18]. But high speed gearing has presented some challenges both to designers and manufacturers [5]. Therefore a better understanding of the loading and analysis of the elements and transmission process in gearing can help in addressing these challenges. Similarly, developing suitable design analysis methods that can be easily applied in practice are necessary in order to maximize the benefits of helical gear transmission in particular and gears in general. Particularly, relatively accurate simplified design analysis methods help to shorten design and development times and thus reduce design project costs. This work is done with the purpose of providing a relatively accurate simplified design analysis methods for helical gears based on contact fatigue. The power loss per mesh in cylindrical gear drives is of the order of 1% [14] which is considered negligible in this study.

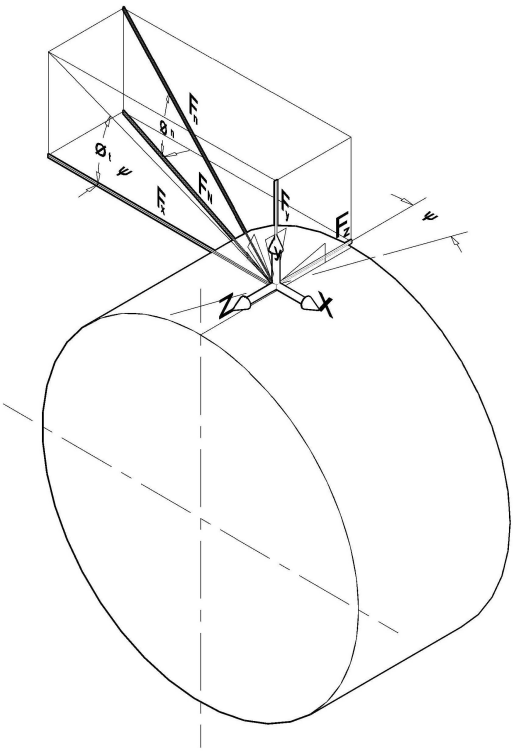

Fig. 1: Forces on helical gear tooth

2. HELICAL GEAR FORCES AND PLANES

Fig. 1 shows the forces on a helical gear tooth at the pitch point on the pitch cylinder. The coordinate axes are set with the pitch point as origin. The driving force is the tangential force F_x but the force F_n determines the contact stress while F_N determines the bending stress on the gear tooth. The pressure angle ϕ_t is different from ϕ_n due to the helix angle of the helical gear teeth.

The relationship between the angles [7] is:

$$\tan\phi_t = \frac{\tan\phi_n}{\cos\psi} \tag{1}$$

The flowing force relations may be verified by referring to standard books in machine design [2, 3, 4, 6, 7, 8]:

$$T_1 = \frac{30P_1 \times 10^3}{\pi N_1} \tag{2}$$

$$F_x = \frac{T_1 \times 10^3}{d_1} \tag{3a}$$

$$F_y = F_x \tan\phi_t \tag{3b}$$

$$F_z = F_x \tan\psi \tag{3c}$$

$$F_N = \frac{F_x}{\cos\psi} \tag{4a}$$

$$F_n = \frac{F_x}{\cos\psi\cos\phi_n} \tag{4b}$$

Fig. 2 shows the common planes often associated with helical gears. The transvers plane is the plane of rotation and is perpendicular to the axial plane. The driving force for the gearset is created in the transverse plane. However, actual contact of gear teeth occurs in the normal plane so the operation of a helical gearset depends on what happens on the normal plane. Perhaps this is why Rortbart and Brown [6] called the normal plane as the plane of action in a helical gearing. The normal plane intercepts the pitch cylinders so that the gear tooth profile generated in it has the same properties as the actual helical gear [6]. The normal plane therefore may be used to define an equivalent spur gear for a helical gear. This is depicted in Fig. 2c which shows the equivalent spur gear pitch diameter as a function of the base helix angle (ψ_b). The base helix angle according to Maitra [8] gives accurate estimate of the radius of curvature of the equivalent spur gear on the normal plane.

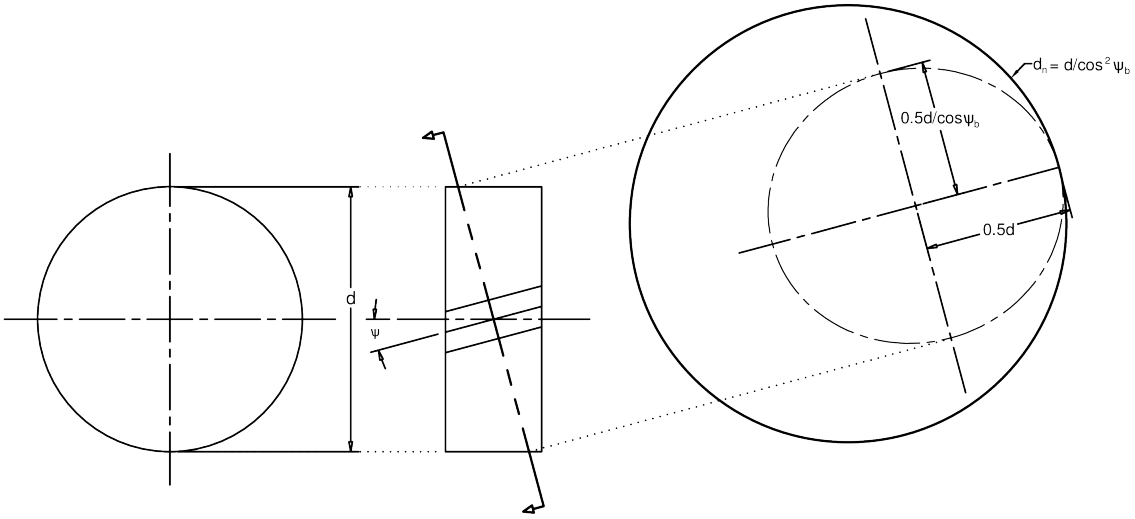

a) Transverse plane b)Axial plane c) Normal plane

Fig. 2: Helical gear planes and equivalent spur gear diameter

The base helix angle may be obtained as [7]:

$$\tan\psi_b = \tan\psi\cos\phi_t \quad (5a)$$

The above equation may be rendered as:

$$\tan\psi_b = \frac{\tan\psi}{\sqrt{1+\tan^2\phi_t}} \quad (5b)$$

For helix angle greater than zero, Eq. (5b) clearly indicates that the base helix angle is smaller. Since the equivalent spur gear size is more accurately estimated by the base helix angle [8], helical gear design models that use the helix angle instead of the base helix angle to estimate the equivalent spur gear size are likely to give results that may be in great error at high helix angles.

As shown in Fig. 2, three planes are commonly associated with helical gears. The transverse and normal planes were briefly described above. The axial plane has the gear support bearings but in helical gears, it can provide additional load shearing for the gear teeth if the face width of a helical gear is greater than the axial pitch. The normal plane has been called the plane of action but it seems to also have a manufacturing advantage over the transverse plane. For the same normal module and normal pressure angle, gears of different helix angles can be made with the same hob. Because hobs can be used to cut different helix angles, spur gear hubs are very often used to generate helical gears up to about 30° helix angle For helical gears less than 1000 mm in pitch diameter, most gear designers will use the same pressure angle and standard tooth size of a spur gear in the normal section of a helical gear [10]. Hence standard spur hob may be used to produce helical gears. In the transverse plane, a different hob is required for different helix angles even for the same transverse module and transverse pressure angle [19]. A shaper cutter is generally needed for each helix angle so helical gears are not often shape generated. When they are shape cut or generated, the shaper tool design is primarily based on the transverse section parameters of the helical gear. Standard spur gear shaper cutters cannot be used to cut helical gears [10].

Fig. 3a is an attempt to graphically illustrate the relationship between the axial directions of a fictitious spur (line OA) and the equivalent spur gear (line OC) of the helical gear with a common origin at O. Line OB is a transition line to line OC. If line OA is drawn to scale to represent the pitch diameter of the fictitious spur gear, then given the base helix angle of a helical gear, one can construct the axial diagram with the

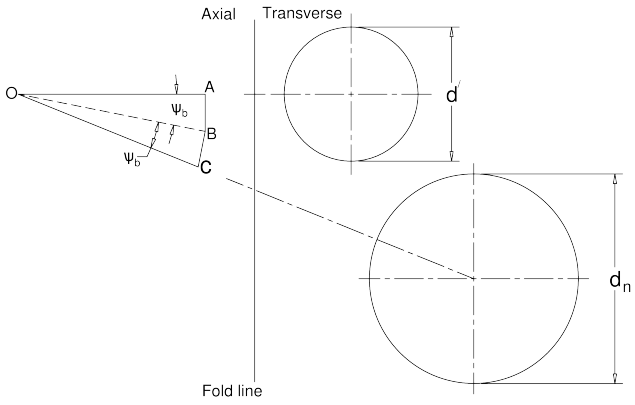

Fig.3a: Axial and transverse planes for equivalent spur gear

length OC representing the pitch diameter of the equivalent spur gear. Note that in the axial diagram, line AB is perpendicular to line OA and line BC is perpendicular to line OB. Also, the angle AOB is equal to angle BOC which is the same as the base helix angle of the helical gear. Now the transverse planes for the fictitious spur and the equivalent spur gears are perpendicular to the respective axial directions and the pitch diameters of the gears may be drawn on these planes as depicted in the transverse plane diagram of Fig. 3a.

The pitch diameters of the fictitious spur and equivalent spur gears are obtained as:

$$d^{/} = zm_n \tag{6a}$$

$$d_n = \frac{d^{/}}{\cos^2 \psi_b} \tag{6b}$$

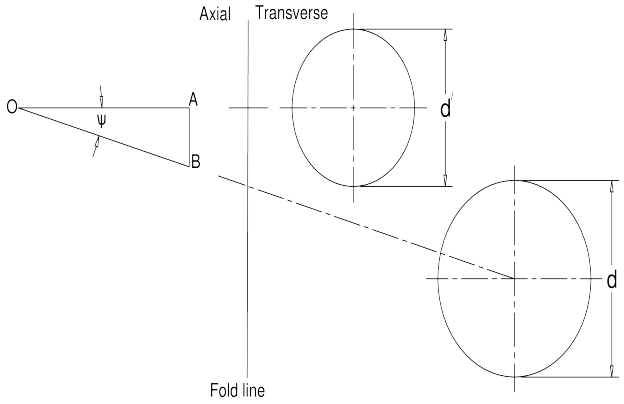

Fig.3b: Axial and transverse planes for helical gear

Fig. 3b is constructed in a similar way to Fig. 3a and the axial directions of a fictitious spur is line OA while line OB is the axial direction of the helical gear with a common origin at O in the axial plane diagram. The transverse planes for the fictitious spur gear and helical gear are perpendicular to the respective axial directions and the pitch diameters of the gears may be drawn on these planes as shown in the transverse plane diagram of Fig. 3b.

The pitch diameter of the helical gear in Fig. 3b is obtained as:

$$d = \frac{d^{/}}{\cos\psi} \tag{6c}$$

The contact ratio of the equivalent spur gearset is:

$$\varpi_n = \frac{\sqrt{(r_{n1} + m_n)^2 - (r_{n1}\cos\phi_n)^2}}{\pi\, m_n \cos\phi_n} + \frac{\sqrt{(r_{n2} + m_n)^2 - (r_{n2}\cos\phi_n)^2}}{\pi\, m_n \cos\phi_n} - \frac{C_n \sin\phi_n}{\pi\, m_n \cos\phi_n} \tag{7}$$

This is approximated as:

$$\varpi_n = \frac{k_1 + k_2}{2\pi \cos\phi_n \cos^2\psi_b} = \frac{\varpi_t}{\cos^2\psi_b} \tag{8}$$

where:

$$\varpi_t = \frac{k_1 + k_2}{\pi \cos\phi_n} \tag{9}$$

Where:

$$k_1 = 0.5\left(\sqrt{(z_1+2)^2 - (z_1\cos\phi_n)^2} - z_1 \sin\phi_n\right) \tag{10a}$$

$$k_2 = 0.5\left(\sqrt{(z_2+2)^2 - (z_2\cos\phi_n)^2} - z_2 \sin\phi_n\right) \tag{10b}$$

The transverse contact ratio ϖ_t of Eq. (9) is for a fictitious spur gear and not the physical helical gear whose transverse plane is inclined at the helix angle from the axis of the fictitious spur gear as indicated in Fig. 3b. It depends on the actual number of gear teeth on the physical helical gearset. The fictitious spur gearset is assumed to have the same number of teeth as the helical gearset and a transverse module equal to normal module of the helical gear. However the transverse contact ratio of the physical helical gear is not directly implied and is not equal to ϖ_t .

Fig. 4 shows the pitches associated with a helical gear. Three pitches: normal, transverse, and axial pitches can be associated with the generating rack. The relationships between the normal and transverses and between the normal and axial pitches are presented. Mathematical derivations of the relationships are available in the references [3, 7, 8], but they can be easily established.

$$p_n = \pi m_n \tag{11a}$$

$$p_t = \frac{p_n}{\cos\psi} = \pi m_t \tag{11b}$$

$$p_z = \frac{p_n}{\sin\psi} = \pi m_z \tag{11c}$$

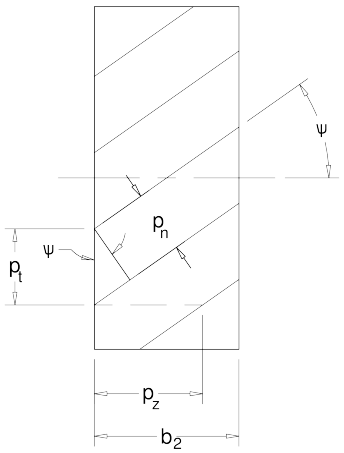

Fig. 4: Pitches of helical gear

From Eqs. (11a) and (11b):

$$m_t = \frac{m_n}{\cos\psi} \tag{12a}$$

From Eqs. (11a) and (11c):

$$m_z = \frac{m_n}{\sin\psi} \tag{12b}$$

3. CONTACT FATIGUE CAPACITY MODEL

During engagement, contact occurs in a gear mesh on two convex surfaces and the contact point would trace out a line if the gear materials and supporting structures were infinitely rigid. Due to material elasticity, the gear teeth deform slightly to form a rectangular contact patch. Kinematically, a gear pair in mesh is analogous to that of a pair of two cylinders of some equivalent diameters, rolling without slipping [8]. Buckingham was the first person to investigate surface stresses in gear teeth in a systematic way [4]. He used the Hertz contact stress expressions for two frictionless cylinders in contact to simulate gear pitting resistance by defining the equivalent radii of curvature of the two cylinders in rolling contact. The equivalent radii of curvature are obtained as the products of the pitch radii of the gearset and the sine of the gear pressure angle. In general, the maximum contact stress for gears in line contact is obtained as [20]:

$$\sigma_H = \sqrt{\frac{F_c E_c \text{x}10^3}{\pi \rho_c\, b}} \tag{13}$$

The composite or contact elastic modulus is obtained as the harmonic mean of the elastic moduli of the contacting cylinders as [20]:

$$E_c = \frac{2E_1E_2}{E_1(1-\upsilon_2^2) + E_2(1-\upsilon_1^2)} \tag{14}$$

In helical gears, contact occurs on the normal plane; therefore the contact force and design geometric parameters should be referred to the normal plane, so we can write:

$$\sigma_H = \sqrt{\frac{F_n E_c \text{x}10^3}{\pi \rho_n\, b_n\, \varpi_n}} \tag{15}$$

The contact ratio, ϖ_n is included in Eq. (15) to account for possible load shearing during gear transmission. Referring to Figs. 2 and 3:

$$\rho_n = \frac{2r_{n2}r_{n1}\sin\phi_n}{r_{n2} \pm r_{n1}} = \frac{d_{n2}\sin\phi_n}{\mu \pm 1} \tag{16}$$

$$r_{n1} = \frac{r_1^{/}}{\cos^2\psi_b};\ d_{n1} = \frac{d_1^{/}}{\cos^2\psi_b} \tag{17a}$$

$$r_{n2} = \frac{r_2^{/}}{\cos^2\psi_b};\ d_{n2} = \frac{d_2^{/}}{\cos^2\psi_b} \tag{17b}$$

Combining Eqs. (16) and (17):

$$\rho_n = \frac{d_2^{/}\sin\phi_n}{(\mu \pm 1)\cos^2\psi_b} \tag{18}$$

$$b_n = \frac{b}{\cos\psi} \tag{19}$$

Substitute Eqs. (4b), (18) and (19) into (15):

$$\sigma_H = \sqrt{\frac{F_x E_c (\mu \pm 1)\text{x}10^3 \cos^2\psi_b}{\pi\cos\phi_n d_2^{/}\sin\phi_n b\,\varpi_t}} = \sqrt{\frac{F_x E_c (\mu \pm 1)\text{x}10^3 \cos^4\psi_b}{d_2^{/} b\,\varpi_t}\left(\frac{2}{\pi\sin 2\phi_n}\right)} \tag{20}$$

Substitute Eq. (3a) into (20):

$$\sigma_H = \cos^2\psi_b \times 10^3 \sqrt{\frac{2K_f(\mu \pm 1)E_c T_1}{\varpi_t b d_1 d_2^{/}}} \tag{21}$$

$$K_f = \frac{2}{\pi\sin 2\phi_n} \tag{22}$$

The involute contact form factor of Eq. (22) may be used to compare the relative load capacities of different standard gear pressure angles. As the gear pressure angle increases, the involute form factor decreases so that gears with higher pressure angles have higher load capacity for the same size. For instance a 20° normal pressure angle gear has $K_f =$ 0.99 (≈1.0), and a 25° normal pressure angle gear has $K_f = 0.831$. This indicates that a 25° normal pressure angle gear has a load capacity of about 20% (100x0.99/0.831) over that of a 20° normal pressure angle gear.

Eq. (21) is explicit in reflecting the principal parameters that determine the Hertz contact stress in helical gears. This brings some simplicity in gear design as the "I" parameter in AGMA model is eliminated. AGMA recommends that the contact stress should be evaluated at the lowest point of single tooth contact (LPSTC) in spur gears because above that point, the load is being shared with other teeth. The AGMA parameter "I" can be computed for LPSTC but is somewhat complicated [14]. Also, Eq. (21) explicitly gives an estimate of the influence of the helix angle on the contact stress capacity of helical gears. Clearly, high helix angles

lead to lower contact stresses and so helical gears would have higher load capacity than spur gears of the same size. Substituting Eq. (6c) for $d_2^{/}$ into Eq. (21), we have:

$$\sigma_H = \cos\psi_b^2 \times 10^3 \sqrt{\frac{2K_f(\mu \pm 1)E_c T_1}{\varpi_t b d_1 d_2 \cos\psi}} \qquad (23)$$

Eq. (23) is the theoretical contact stress capacity model of a helical gear based on its spur gear equivalency. Two issues need be addressed to convert it to a practical or engineering model. These are load shearing during transmission and the actual transmitted load. Load shearing is expected in helical gearsets but as in normal contact spur gears, load shearing will not be exactly equal to the transverse contact ratio. Similarly the load shearing in the equivalent spur gear model will not be exactly equal to ϖ_t . Therefore, we shall substitute ϖ_s for ϖ_t as load shearing factor in the above formula. The actual transmitted load is known from experience to be greater than the rated transmitted load. This is because manufacturing tolerances, elastic deformation of machine elements and supporting structures, local accelerations and decelerations of gear drives, external dynamics of devices coupled with gear drives, foundation vibrations, etc. induce vibrations on meshing gears that magnify the rated transmitted load. Therefore, to account for the load increases on the rated transmitted load in practice, a service load factor K_s will be introduced into the theoretical model. Consequently the engineering contact stress capacity model of a helical gear is:

$$\sigma_H = \cos\psi_b^2 \times 10^3 \sqrt{\frac{2K_s K_f(\mu \pm 1)E_c T_1}{\varpi_s b d_1 d_2 \cos\psi}} \qquad (24)$$

For acceptable design:

$$\sigma_H \le S_H \qquad S_H = \frac{S_c}{n_H} \qquad (25)$$

4. DESIGN SIZING BASED ON CONTACT FATIGUE

The objective in design sizing is to obtain initial estimate of a component size based on specific serviceability criteria. In gear design, contact fatigue (pitting) and bending fatigue failures are the most commonly used serviceability criteria. We are concerned here only with pitting resistance sizing. Gear design is an iterative process and the initial solution provides trial values of gear sizes. The basic gear size parameter is the module, therefore finding an initial module value constitutes gear design sizing.

Now from Eq. (5):

$$d_1 = \frac{z_1 m_n}{\cos\psi} \qquad (26a)$$

$$d_2^{/} = z_2 m_n \qquad (26b)$$

$$b = \lambda_b d_1 = \frac{\lambda_b z_1 m_n}{\cos\psi} \qquad (26c)$$

Sub substituting Eq. (26) into Eq. 24 to obtain:

$$\sigma_H = \sqrt{\frac{2K_f K_s(\mu \pm 1)E_c T_1 \text{ x}10^6 \cos^4\psi_b \cos^2\psi}{\lambda_b \mu \varpi_s z_1^3 m_n^3}} \qquad (27)$$

From a sizing perspective:

$$\sigma_H \le S_H \qquad (28)$$

Hence by combining Eqs. (27) and (28):

$$m_n \ge \frac{100}{z_1}\left[\frac{2K_f K_s(\mu_o \pm 1)E_c T_1 \cos^4\psi_b \cos^2\psi}{\lambda_b \mu \varpi_s S_H^2}\right]^{\frac{1}{3}} \qquad (29)$$

In Eq. (29), the design speed ratio μ is replaced with the desired speed ratio μ_o because the former is unknown at the beginning of a gear design problem, but the latter is either specified or can be determined. Since $\psi > \psi_b$ for any helix angle greater than zero, a conservative solution from Eq. (29) for the normal module is obtained by setting $\cos\psi = \cos\psi_b$. That is:

$$m_n \ge \frac{100\cos^2\psi_b}{z_1}\left[\frac{2K_f K_s(\mu_o \pm 1)E_c T_1}{\lambda_b \mu \varpi_s S_H^2}\right]^{\frac{1}{3}} \qquad (30)$$

Now, the service factor K_s (Eq. 42) is generally a function of the pitch velocity and gear sizes through the parameters K_v , K_m and K_r . Since gear sizes are not kwon at the beginning of the design process, we need an initial estimate of K_s . The external overload factor K_o can be selected based on the drive characteristics of the power source and driven devices. An approximate initial value of K_m based on Schmid, Hamrock & Jacobson [21] and Osakue & Anetor [22] but slightly modified for helical gears is:

$$K_m^{/} \approx 1 + 0.93\lambda_b\left[0.20 + 0.0112\left(\frac{2K_o T_1}{\lambda_b}\right)^{1/3}\right] \qquad (31a)$$

Eq. (31a) clearly shows the dependence of K_m on the rated load, T_1 and so is K_v because it depends on the tangential speed and gear tooth quality number. The gear tooth quality number is often selected based on the tangential velocity which is determined by the gear pitch diameter and its rotational speed. It is thus suggested that an initial estimate of K_v may be taken as:

$$K_v^{/} \approx 2K_m - 1 \tag{31b}$$

Then load service factor for design sizing may be estimated as:

$$K_s^{/} \approx K_o K_v^{/} K_m^{/} \tag{31c}$$

Hence, Eq. (30) reduces to:

$$m_n \geq \frac{100\cos^2\psi_b}{z_1}\left[\frac{2K_f K_s^{/}(\mu_o \pm 1)E_c T_1}{\lambda_b \mu_o \varpi_s S_H^2}\right]^{\frac{1}{3}} \tag{32}$$

Eq. (32) avoids the need to specify the gear tooth quality which depends on pitch line velocity. The gear tooth quality choice can now be made during design verification when basic gear dimensions are known. However, it requires the choice of a gear material and surface hardness at the sizing phase so as to estimate the design contact fatigue strength. This is not a real challenge even to a novice gear design as common gear materials can easily be researched. Materials and hardness can be varied during design verification in order to explore alternatives.

In choosing the number of teeth on pinion, interference must be avoided. In reference [3], the smallest number of helical pinion teeth of standard ISO tooth proportion that can run with a rack without interference is given. Sometimes, the gear ratio is considered when choosing the number of teeth for the pinion [20]. Gear ratio in single-helix gearsets can be up to 10 and may be up to 15 or 20 in double-helix gearsets [6, 18]. In view of the above and for speed-reducing drive with $\mu_o \leq 15$, it is suggested that:

$$z_1 = \max\left(\frac{2\cos\psi}{\sin^2\phi_t},\ 26 - 1.25\mu_o\right) \tag{33}$$

The shape factor largely depends on accuracy of gear manufacture and assembly. A tentative maximum value of λ_b for medium-hard gears may be estimated as:

$$\lambda_b \approx 0.275 + \frac{0.8\mu_o}{\mu_o + 1} \tag{34}$$

Eqs. (33) and (34) allow us to provide initial values of these parameters in Eq. (32) in order to estimate the normal module. Thereafter, a standard normal module value is chosen and the helical gearset basic dimensions are determined. The number of gear teeth is estimated as:

$$z_2 \approx \mu_o z_1 \tag{35a}$$

An integer value for z_2 must be chosen. Then refine:

$$\mu = \frac{z_2}{z_1} \tag{35b}$$

Choosing a higher normal module value than estimated allows a designer to reduce z_1 and z_2 while keeping μ constant. When a hunting tooth is used in power drives, the speed ratio error or tolerance should be checked. That is:

$$\in_o = \frac{100(\mu_o - \mu)}{\mu_o} \tag{36}$$

When $\in_o$ is acceptable, then:

$$d_1 = \frac{m_n z_1}{\cos\psi} \tag{37a}$$

$$d_2 = \frac{m_n z_2}{\cos\psi} \tag{37b}$$

$$C = \frac{d_1 + d_2}{2} = \frac{m_n(z_1 + z_2)}{2\cos\psi} \tag{37c}$$

$$b_2 = \lambda_b d_1 \tag{38a}$$

$$\varpi_f = \frac{b_2 \sin\psi}{\pi m_n} \geq 1.15 \tag{38b}$$

$$b_1 \leq b_2 + 5\,\text{mm} \tag{39}$$

5. LOAD SHEARING FACTOR IN EQUIVALENT SPUR GEAR

In spur gears with transverse contact ratio less than 2, the load shearing factor is taken as unity because a pair of gear teeth bears the transmitted load around the pitch circle. Since a helical gearset is represented by its equivalent spur gearset in the new model, it would seem appropriate to assume a load shearing factor of unity in helical gearset with transverse contact ratio less than 2 as in standard spur gears. However, we must note the following: a) the transverse contact ratio developed in our model is not for the physical helical gear transverse plane but for a fictitious spur gear; b) the equivalent spur gear model ignores facial overlap in actual

helical gears when gear face width is more than one axial pitch; c) due to the influence of the helix angle in Eq. (23) it may be argued that some of the load shearing effect is somewhat incorporated in the model. However, it is unlikely that this can sufficiently account for the total load shearing which always exist in helical gears. Thus ignoring load shearing completely would appear to be too conservative.

Generally, load sharing in gear transmission can be enhanced by wear-in and accurate manufacture of gear teeth. Low manufacturing accuracy and high hardness of gear teeth reduces load sharing. Inaccurate low-hardness gears may wear-in and cold-flow enough to develop relatively good contact patterns and load shearing early in their service life. Usually, helical and bevel gears are made accurate enough for load sharing to occur [10]. In helical gears, the load shearing factor is the ratio of the face width to the minimum total length of the contact lines. AGMA provides methods for its estimation but they are rather involved processes [7]. Such methods may be necessary for detail or prototype design and should be done by gear specialists. However, AGMA also has an approximate method which uses the transverse contact ratio of the helical gear (not the fictitious spur gear) that is factored by an effective face width coefficient of 0.95. Since the helix angle influence is more pronounced in the model presented, it must be admitted that a load shearing factor smaller than that of AGMA is desirable. In preliminary gear design, simplified empirical estimates may be used. So taking a clue from the AGMA approximate method, we suggest that:

$$\varpi_s = 0.5(1+\varpi_t) \tag{40}$$

6. HELIX ANGLE APPROXIMATION ERROR

In Eqs. (24) and (32), the function $\cos^2\psi_b$ captures the direct influence of the helix angle on the contact stress and normal module size. The base helix angle (ψ_b) according to Maitra [8] gives accurate estimate of the radius of curvature of the equivalent spur gears on the normal plane of contact. But majority of the current available models for helical gears use the helix angle (ψ) in design analysis. We have used the base helix angle (ψ_b) so as to formulate a simplified but reasonably accurate model. Specifically in Eq. (29), the preference of the base helix angle is informed by design practice which has a bias for conservatism. Using ψ in this equation would mean smaller normal module size. It was felt informative to investigate the error that may be expected in our approximation using the error function:

$$\in_{\psi} = \frac{100(\cos^2\psi_b - \cos^2\psi)}{\cos^2\psi_b} \tag{41}$$

The error function is plotted in Fig. 5 against the helix angle. It is clear from this figure that for low helix angles of $\psi \le 20^o$, the error in using ψ instead of ψ_b is about 2.5% which is considered negligible. The error grows exponentially beyond 20^o. This shows that using the base helix angle in our model is conservative and probably more realistic.

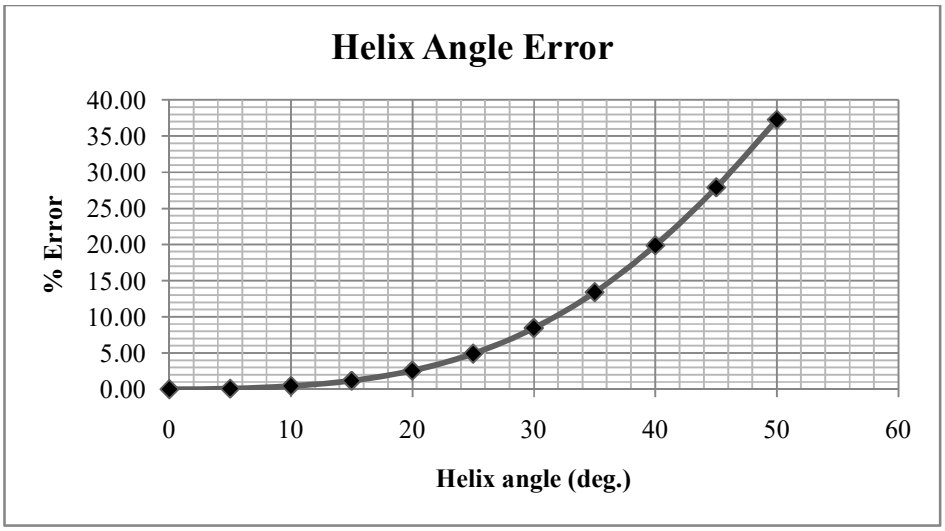

Fig. 5: Helix angle error plot

7. SERVICE LOAD FACTOR

Actual loads on equipment in service vary to different degrees depending on the environment, application, assembling accuracy, and proper installation. Experience shows that the forces acting on equipment in service are generally higher than the rated or nominal values. These higher values may be due to mechanical defects and or imperfections in manufacturing, assembling, installations, and operations. In addition, elastic deformations of machine components and supporting structures during operations and wear from rubbing surfaces create vibrations that increase the rated loads. Generally, tolerances on machine components are necessary due to manufacturing imperfections but tolerance stack-up can lead to looseness in assemblies. Sometimes clearances are required for functional reasons as in journal bearings and looseness cannot be avoided in such cases. Loosely tied-down foundations, loose bearing restraints, and excessive bearing clearances increase service loads because

of associated vibrations when devices are in operations. Unbalance of rotating parts which can be due to manufacturing and assembling imperfections leads to vibration also. Misalignment during assembling operations creates additional sources of overload. In the light of the above, rated transmitted load can hardly be the same as the actual transmitted or service load. Hence the service load is generally a magnification of the rated transmitted load. However, the actual load capacity of a gearset can be determined reliably only by practical experimentation [8].

Practically, the design or service load is often estimated by multiplying the rated load with an overload or service load factor. The service load factor is used to account for load increases during normal operations of the gearset. It takes care of load excitations beyond the rated value that are reoccurring in nature and represents a magnification factor for the rated load in a gear design problem. It may be evaluated by a multiplicative model as [20]:

$$K_s = K_o K_v K_m K_r K_c \tag{42}$$

The service load factor of Eq. (42) accounts for different conventional rated load modifiers in gear design. The external overload factor K_o takes care of possible overloading due to the dynamics of the power source and driven devices. The values are based on industry experience and recommendations are available in gear standards. The internal overload factor, K_v accounts for load excitations from manufacturing inaccuracies due to non-conjugate actions of meshing gear teeth, backlash, profile, pitch, errors, etc. and dynamic imbalance. The value of K_v is based on the pitch point speed in AGMA standard which given by:

$$V_t = \frac{\pi N_1 d_1}{60{,}000} \tag{43}$$

Since wide-face helical gears run more quietly than spur gears [3], this suggests that the value of K_v for wide-face helical gears should be somewhat lower than those of spur gears. It should therefore, be conservative to use values of K_v for spur gears in helical gear design. Because narrow-face helical gears make about the same noise as spur gears [3], then the values of K_v for narrow-face helical gears should be about the same as spur gears. The mesh overload factor, K_m accounts for non-uniform spread of the transmitted load across the gear face width of a meshing gears due to misalignment of gears and shafts caused by dynamic twisting and bending. The rigidity factor K_r accounts for vibrational overload associated with the gear tooth base support flexibility. The rigidity factor is assessed by the rim backup ratio which is defined as the rim thickness divided by the whole depth of gear tooth. K_c takes care of the quality of the contact mesh and [20] suggests a value of 1.1 for K_c for spur gears. AGMA [23] provides methods for estimating K_v, K_m, and K_r.

8. MESH OVERLOAD FACTOR (K_m)

The mesh overload factor in gear design accounts for non-uniform spread of the transmitted load across the face width of a meshing gear. It depends on the accuracy of mounting, bearings, shaft deflection and accuracy of gears. Maintaining uniform loading across the face width of gear tooth is difficult during operations. Misalignment due to elastic deformation of gears, supporting elements and structure causes mismatch of gear teeth leading to non-uniform mesh load distribution which increases the mesh overload factor. Gear teeth mismatch is less for gears with smaller face width but to minimize the problem, the face width-pinion diameter ratio called aspect ratio or shape factor may be limited. For instance API standards recommend limits on aspect ratio (includes gap in double-helix gears) in certain applications and require gear manufacturers to submit detail analysis when exceeded [16]. Dynamic bending and twisting have no serious effects on straddle mounted single-helix gears with shape factor less than 1.15 [10]. When a single-helix pinion and a double-helix pinion have the same working face width, the mesh overload factor tends to be the same in value [10]. High mesh overload factor may be reduced through helix correction and should be given serious consideration when the shape factor exceeds 1.15 for single-helix gears and 1.6 for double-helix gears and values above 2.0 are uncommon [10]. Cantilever mounted gears may have serious dynamic bending and twisting even with shape factors less than unity. A small shape factor gives less dynamic twisting and bending of the pinion but higher shape factors minimize pitch point speed [16]. The mesh overload factor for helical gears is about 93% of spur gears due to slight insensitivity of helical gears to mesh misalignment [24]. That is:

$$K_m = 0.93 K_m' \tag{44a}$$

The practical range of K_m' is from 1.0 to 2.0 [4], indicating values of at least 1.0. To avoid a mesh overload factor less than unity from Eq. (44a) for helical gears, we suggest that:

$$K_m = 1 + 0.85(K_m' - 1) \tag{44b}$$

9. CONTACT FATIGUE MODEL APPLICATIONS

The equations presented in the previous sections were coded in Microsoft Excel for computational efficiency. The spreadsheet has two pages of two sections per page. The first page has a material selection and strengths estimation sections. The material selection part helps in specifying gearset materials and the surface and core hardness or heat treatment. It then determines the nominal contact and bending fatigue strengths. The second part of the first page determines the strength modification factors, and estimates both design contact and bending fatigue strengths. The second page has

design sizing and design verification sections. The design sizing for pitting resistance determines an estimate of gear normal module based on contact resistance and allows a choice of a standard gear module. The design verification section uses the chosen gear normal module to determine gearset basic dimensions, evaluate service load factor and nominal strength modification factors, and determines the expected contact stress. It then assesses design adequacy through the contact stress design factor. Iteration during design verification can be done by changing the value of effective face width, gear module, and gear teeth. The gear pitch diameter is changed when either the module or gear teeth number is changed.

The new design contact stress capacity model presented in the previous section is tested in five design Examples which involve determination of contact stress, a design verification task. The sixth Example determines the basic dimensions of a gearset (design sizing task) and checks the adequacy of the design in design verification. Example 6 demonstrates how the new contact fatigue capacity model is used in both design sizing and design verification tasks. The problem statements in the Examples have been paraphrased and the design parameters have been converted to metric units by the authors.

Example 1: A 17-tooth helical steel pinion with a right-hand helix angle of 30^o rotates at 1800 rpm when transmitting 3 kW to a 52-tooth helical steel gear. The gearset has a normal pressure angle of 20^o, normal module of 2.54 mm, and a face width of 38.1 mm. Determine the contact stress on the gear pairs for a service load factor of 1.769 [3, p. 771 – 773].

Example 2: A 15-tooth helical steel pinion with a right-hand helix angle of 41.41^o rotates at 2500 rpm when transmitting 3.75 kW to a 24-tooth helical steel gear. The gearset has a normal pressure angle of 20^o, normal module of 2.54 mm, and a face width of 29.21 mm. Determine the contact stress on the gear pair for a service load factor of 1.84 [2, p. 658 – 662].

Example 3: A helical steel gearset for a milling machine drive is to transmit 48.5 kW from an electric motor with a pinion speed of 3450 rpm and a gear speed of 1100 rpm. The gearset has a normal pressure angle of 20^o and a helix angle of 15^o. The pinion has 24 teeth, gear has 75 teeth, the normal module is 2.17 mm and the face with is 58.15 mm. Determine the contact stress on the gear pair for a service load factor of 2.552 [14, p. 461 - 462].

Examples 4 & 5: A 3-helical steel gear train transmits 15 kW at 2500 rpm at the pinion. The pinion has 14 teeth, idler has 17 teeth and the gear has 49 teeth. The gearset has a normal pressure angle of 25^o, helix angle of 20^o, normal module of 4.233 mm, and face width of 67.74 mm. Determine the contact stresses on the gear pairs for a service load factor of 2.424 [4, p. 764 - 768]. Note that two gearsets are involved in this problem: pinion-idler (Example 4), and idler-gear (Example 5) combinations.

9.1 Solutions: Examples 1 to 5

Table 2 summarizes the basic gearset dimensions and load data for Examples 1 to 5. AGMA contact stresses were evaluated using a new version of the model, so some of the AGMA results shown in our results are slightly different from those in the references. The newer AGMA model gives less conservative results. Table 3 shows the AGMA contact stress values in column 2 and the new model contact stress values in column 3. The percentage difference between the new contact stress capacity model values and AGMA values are indicated in column 4. The variances between the results are in the range of -10% to 6% in the wide range of helix angles which span 15^o to 41.41^o. Clearly the new model appears to compare favorably with AGMA model results. According to Matthew [25], simplified engineering models can yield ±10% accuracy. From the favorable comparison of the five Examples presented with AGMA model, it seems reasonable to accept the new model for preliminary design which is tested in Example 6.

Table 2: Input Parameters for Contact Stress for Examples 1 to 5

Parameters	Example				
	1	2	3	4	5
Transmitted power (kW)	3	3.75	48.5	15	15
Pinion speed (rpm)	1800	2500	2450	2500	2056
Pinion torque (Nm)	15.92	14.32	134.24	57.30	69.67
Speed ratio	3.0	1.60	3.136	1.216	2.884
Normal pressure angle (^{o})	20	20	20	25	25
Helix angle (^{o})	30	41.41	15	20	20
Normal module (mm)	2.54	2.54	2.17	4.233	4.233
Pinion teeth number	17	15	24	14	17
Gear teeth number	51	24	75	17	49
Pinion pitch diameter (mm)	49.86	50.8	53.92	63.07	76.58
Gear pitch diameter (mm)	149.58	81.28	168.49	76.58	220.73
Face width (mm)	38.1	24.13	57.15	67.74	67.74
Service load factor	1.769	1.840	2.472	2.424	2.424

Table 3: Contact Stresses for Examples 1 to 5

Example	Face Contact Ratio	Contact Stress (MPa)		
		AGMA	New Model	Difference (%)
1	2.39	296.51	300.29	-1.27
3	2.00	363.07	340.99	6.08
4	2.17	852.40	887.44	-4.11
5	1.74	497.74	543.92	-9.27
5	1.74	377.21	416.27	-10.35

Example 6: A pair of helical steel gears is to transmit 8.5 kW from an electric motor with the pinion running at 720 rpm and the gear at 144 rpm. The normal pressure angle is 20^o while the helix angle is 20^o. The gears are made from carbon steel material and are each thru-hardened to 300 HVN. Design the gearset for a minimum life of 10^8 load cycles based on 99% reliability. Assume an external overload factor of 1.5.

Solution: A minimum life of 10^8 load cycles implies the slower running gear should last at least 10^8 load cycles. This information was used to determine the design contact strength of the gearset, indicating that the pinion is weaker, with estimated design contact strength of 739 MPa. Gear design contact strength was determined on the basis of AGMA recommendations. AGMA gear material nominal strength data are determined at 99% reliability at 10^7 load cycles. Nominal strengths are usually determined experimentally in controlled environments. For field applications, the nominal strengths need adjustments, so AGMA [23] recommends several factors as modifiers.

Table 4 shows design sizing parameters. Design sizing estimates yielded pinion teeth number of 19, gear teeth number of 95, and normal module value 3.28 mm based on pitting wear resistance. A standard normal module value of 3.5 mm [14] was chosen. Table 5 shows the design verification data for the first iteration which yielded acceptable results because a design factor of 1.18 is obtained against a desired value of 1.1. The service load factor estimate for design sizing is 2.514 based on a shape factor of 0.78. The corresponding value for design verification based on a shape factor of 0.75 is 2.506. These two values are very close, the difference being only 0.3%.

Table 4: Design Sizing for Example 6

Parameter	Value
Transmitted power (kW)	8.5
Pinion rotational speed (rpm)	720
Pinion rotational speed (rpm)	144
Desired speed ratio	5
Pinion number of teeth	19
External overload factor	1.50
Composite elastic modulus (GPa)	230
Pinion torque (Nm)	112.73
Surface hardness (HVN)	300
Design contact strength (MPa)	739
Desired design factor	1.10
Service load factor	2.514
Normal module (mm): estimate	3.28
Normal module (mm): chosen	3.50

Table 5: Design Verification for Example 6

Parameter	Value
Normal pressure angle (^{o})	20
Helix angle (^{o})	20
Gear normal module (mm)	3.50
Pinion teeth	19
Gear teeth	95
Design speed ratio	5
Pinion pitch diameter (mm)	70.77
Gear pitch diameter (mm)	357.56
Pinion face width (mm)	50
Face contact ratio	1.56
Service load factor	2.506
Contact stress (MPa)	628.17
Estimated design factor	1.18

10. CONCLUSION

A simplified contact stress capacity model that is explicit in the representation of helical gear design parameters is presented. The model gives estimate of the contact stress expected in a helical gear mesh. Five design Examples of contact stresses from different references are computed and they compare very favorably with AGMA estimates because the percentage variances between the two model values are in the range of -10% to 6% in the Examples. It is important to note the wide range of the helix angle which spans 15^o to 41.41^o and the different normal pressure angles of 20^o and 25^o in the Examples considered. Secondly, the new model appears to give slightly higher contact stress values in general so that for preliminary design, it offers the advantage of providing conservative solutions. The favorable comparison should give some confidence in using the new model for preliminary design tasks of helical gears. Generally, higher helix angle leads to lower contact stress and smaller normal module size. Therefore, helical gears have higher load capacity compared to spur gears of the same size because a spur gear may be considered as a helical gear with helix angle of 0^o.

The new contact stress capacity model was modified for design sizing and its application is demonstrated in Example 6. Design sizing provides the value of gear normal module based on contact fatigue or pitting resistance which is used to determine the other basic dimensions of a gearset. Comparison of the service load factor values for design sizing and design verification indicates a difference of only 0.9% in Example 6. This is a very close prediction which though cannot be generalized nonetheless recommends the design method presented. While more Examples are necessary for

further verification of the design approach presented, it may however, be concluded from the results of the design Examples considered that the approach is sufficiently accurate enough to be acceptable for preliminary design of helical gears. This model may be used for spur design if the helix angle is taken as 0^o.

ACKNOWLEDGEMENTS

The authors gratefully acknowledge that this study was supported in parts with funds from COSET Research Fund and the University Faculty Development Fund of Texas Southern University, Houston, Texas.

NOMENCLATURE

HBN = Hardness: Brinnel Number
HRC = Hardness: Rockwell C-scale
HVN = Hardness: Vicker's Number
HPSTC = Highest Point of Single Tooth Contact
b = effective gear face width (mm)
b_1 = pinion face width (mm)
b_2 = gear face width (mm)
b_c = effective contact width on of cylinder (mm)
b_n = effective gear face width on normal plane (mm)
C = center distance of helical gears (mm)
C_n = center distance of equivalent spur gears (mm)
C_p = AGMA gearset material factor
$d^{/}$ = pitch circle diameter of fictitious spur pinion or gear (mm)
d_n = theoretical pitch circle diameter of equivalent spur pinion or gear (mm)
d = pitch circle diameter of helical pinion or gear(mm)
E = elastic modulus of pinion or gear (GPa)
E_c = composite contact elastic modulus (GPa)
F_n = normal contact force (N)
F_N = normal bending force (N)
F_x = rated transmitted or transverse force (N)
F_y = rated radial force (N)
F_z = rated axial force (N)
I = AGMA pitting geometric factor
k_1 = pinion action line factor
k_2 = gear action line factor
K_f = gear form factor
$K_s^{/}$ = sizing service load factor
$K_m^{/}$ = mesh overload factor for spur gear or sizing value for helical gear
$K_v^{/}$ = sizing internal overload factor
K_s = service load factor
K_o = external overload factor
K_v = internal overload factor
K_m = mesh overload factor
K_r = rim rigidity factor
K_c = contact quality factor
m_t = transverse module of gear (mm)
m_n = normal module of gear (mm)
m_z = axial module of gear (mm)
n_H = design factor for surface strength
n_F = design factor for bending fatigue strength
N = rotational speed of pinion or gear (rpm)
P = power at pinion or gear (kW)
q_n = gear tooth quality number
r = radius of pinion or gear (mm)
T = rated torque at pinion or gear (Nm)
$S_c^{/}$ = nominal design contact fatigue strength
S_c = design contact fatigue strength
S_H = allowable contact fatigue stress (MPa)
V_t = tangential velocity at pitch point (m/s)
Y_{cs} = contact fatigue strength adjustment factor
Y_{cn} = contact fatigue durability factor
Y_{cz} = contact fatigue size factor
Y_{co} = oil temperature factor
Y_{cr} = contact reliability factor
Y_h = gear hardness factor
z = number of teeth on pinion or gear
Z_c = number of contacts per revolution
Z = length of path of action in transverse plane
υ = Poisson's ratio of pinion or gear
ρ_n = normal plane radius of curvature of gear at pitch point of pinion or gear (mm)
ρ_c = composite radius of curvature at pitch point for spur gear (mm)
ϕ_t = transverse pressure angle (deg.)
ϕ_n = normal pressure angle (deg.)
ψ = helix angle (deg.)
ψ_b = base helix angle (deg.)
μ = design speed ratio
μ_o = desired speed ratio
ϖ_n = normal plane contact ratio

ϖ_t = transverse plane contact ratio

ϖ_f = face or axial contact ratio

ϖ_s = load sharing factor

ϖ_T = AGMA load sharing ratio

σ_H = maximum Hertz contact stress (MPa)

$\in_\psi$ = helix angle error

$\in_o$ = speed ratio error

λ_b = gear aspect ratio or face width factor

1 = subscript for pinion

2 = subscript for gear

REFERENCES

[1] Khurmi, R. S. & Gupta, J. K., A Textbook of Machine Design, Eurasia Publishing House, New Delhi.

[2] Collins, J. A., Busby, H., Staab, G. H., (2010), *Mechanical Design of Machine Elements and Machines: A Failure Prevention Perspective*, 2nd ed., John Wiley and Sons, New York.

[3] Budynas, R. G. & Nissbett, J. K., Shigley's Mechanical Engineering Design, 9th ed., McGraw Hill Education.

[4] Norton, R. L. (2000), *Machine Design: An Integrated Approach*, Prentice-Hall, Upper Saddle River, New Jersey.

[5] Partridge, J. R., *High Speed Gears-Design and Applications*: http://turbolab.tamu.edu/proc/turboproc/T6/T6pg133-142.pdf

[6] Rortbart, H. A. & Brown, T. H. (2006), *Mechanical Design Handbook*, 2nd ed., McGraw-Hill, New York.

[7] Shigley, J. E and Mischke, C. R. (Chief Editors), (1996), Standard Handbook of Machine Design, McGraw-Hill, New York.

[8] Maitra, G. M., (2013), *Fundamentals of Toothed Gearing: Handbook of Gear Design*, 2nd ed., McGraw Hill, New Delhi.

[9] Bhandari, V. B. (2010), *Design of Machine Elements*, 3rd ed., McGraw Hill, India, p. 370.

[10] Dudley, D. W. (2009), *Handbook of Practical Gear Design*, CRC Press, Baca Raton.

[11] Schmid, S. R., Hamrock, B. J. & Jacobson,B. O., (2014), *Fundamentals of Machine Elements*, 3rd ed., CRC Press, New York.

[12] Bergseth, E. (2009), *Influence of Gear Surface Roughness, Lubricant Viscosity and Quality Level on ISO 6336 Calculation of Surface Durability*, Technical Report, Department of Machine Design, Royal Institute of Technology, Stockholm, https://www.diva-portal.org/smash/get/diva2:489751/FULLTEXT01.pdf (Accessed 2-20-16)

[13] Savage, M. & Mackulin, M. J. (1991), *Maximum Life Spur Gear Design*, NASA Technical Memorandum 104361. http://www.dtic.mil/dtic/tr/fulltext/u2/a237143.pdf (2-3-16)

[14] Mott, R. L. (2004), *Machine Elements in Mechanical Design*, 4th ed. SI, Pearson Prentice Hall, New York.

[15] Industrial Wiki, *Gear Drives*: http://www.myodesie.com/index.php/wiki/index/returnEntry/id/3000

[16] Beckman, K. O., & Patel, V. P. *Review of API Versus AGMA Gear Standards-Rating, Data Sheet Completion, and Gear Selection Guidelines*, pp. 191 – 204

[17] Gidado, A. Y., Muhammad, I., & Umar, A. A., (2014), Design, Modeling and Analysis of Helical Gear According to Bending Strength Using AGMA and ANSYS. Int'l Journal of Engineering Trends and Technology, Vol. 8, No 9.

[18] RoyMech, Helical Gears: http://www.roymech.co.uk/Useful_Tables/Drive/Helical_Gears.html

[19] *Gear Technical Reference - KHK Gears,* http://khkgears.net/wp-content/uploads/2015/10/gear_guide.pdf. p. 615.

[20] Osakue, E. E., (2016), Simplified Spur Gear Design, Proceedings of International Mechanical Engineering Congress and Exposition 2015, Paper Number IMECE2016-65426, November 11-17, Phoenix Arizona, USA.

[21] Schmid, S. R., Hamrock, B. J. & Jacobson, B. O., (2014), *Fundamentals of Machine Elements*, 3rd ed., CRC Press, New York.

[22] Osakue, E. E. and Anetor, L. (2016), Spur Gear Design: Some New Perspectives, Int'l Journal of Research in Engineering and Technology, Vol. 5, Is. 7, pp. 275 - 286.

[23] AGMA 2001-D04, *Fundamental Rating Factors and Calculation Methods for Involute Spur and Helical Gear Teeth*: http://wp.kntu.ac.ir/asgari/AGMA%202001-D04.pdf

[24] Gopinath, K. & Mayuram, M. M., *Module 2 Gears, Lecture 11, Helical Gears:* http://nptel.ac.in/courses

[25] Matthews, C. (2005). *ASME Engineer's Data Book,* 2nd ed. ASME Press.

[26] Lawson, E., *New ANSI/AGMA Accuracy Standards for Gears - Gear-ANSI/AGMA 2015-1-A01*; www.geartechnology.com/issues/0304/lawson.pdf

APPENDIX

Steel Gear Material Manufacturing Grades

Steel is the most widely used gear material and could be low-carbon, low-alloy to high-carbon, high-alloy types. When cost is of major importance in material selection, low-carbon or low-alloy steel materials are most attractive. If small size and high power transmission capacity are major factors in design, then high-carbon or high-alloy steel materials are most attractive. Steel gear materials can be made to three manufacturing grades of 1, 2, and 3; according to AGMA standards [ANSI/AGMA 2001-D04]. Higher grade numbers mean higher quality steels which can be used for higher load capacity. Thru-hardened and induction hardened or flame

hardened gears can normally be obtained in grades 1 and 2 while case-hardened (carburized and nitrided) gears can be obtained in all three grades.

Gear Tooth Quality

Gear tooth quality is representative of the manufacturing perfection of gear tooth profile and is indicated by quality number assigned by ISO/AGMA. The gear tooth quality numbers range from 0 to 12 with lower numbers representing higher gear quality. Cast, forged, and pressed gears will roughly be of gear quality numbers 10 to 12, form cut gears about 9 to 10, shaped or hobbed gears of 8 to 9, shaped or hobbed and fine finished gears of 6 to 7, shaped or hobbed and ground gears of 4 to 5 quality numbers [8]. Hobbing can produce quality numbers of 10 to 7, shaved gears can have 8 to 6 quality numbers and ground gears can have 7 to 2 quality numbers. The most popular gear quality numbers are 6 to 9. Gears of tooth quality numbers 5 and below are for very accurate gearing. Quality number values should be selected based on experience [26]. Table A1 is suggested as a general guide.

Table A1: Gear Tooth Quality Number for Pitch Speed

Pitch Velocity (m/s)	Gear Tooth Quality Number (q_n)
0 - 3	12 - 10
3 - 7	10 - 9
6 - 10	9 - 8
10 - 15	8 – 6
> 15	< 6

Gear Assembly Classes

Proper operation and performance of gear drives not only depend on design and manufacturing, but on the quality of its assembly identified by classes. The assembly class is dependent on the assembly tolerances and rigidity of the supporting elements and structure. Gear drive assembly classes may be described as open, commercial enclosed, precision enclosed, and extra-precision enclosed drives, according to AGMA.

a) Open Drives: This refers to gear drives where shafts are supported in bearings that are mounted on structural elements of machines that can allow relatively large misalignment. Such drives are found in low-speed non-critical drives, hand-operated drives, etc.
b) Commercial Enclosed Drives: The bearings of these drives are mounted on specially designed housings that have more rigidity than open drives. However, tolerances on individual dimensions are fairly loose.
c) Precision Enclosed Drives: The housing and supporting structures of these gear units are made to tighter tolerances than commercial enclosed drives.
d) Extra-precision Enclosed Drives: The housing and supporting structures of these gear units are made to exacting precision and are often adjusted at assembly to achieve excellent alignment of gear teeth.

Estimating Design Contact Strength

Contact fatigue strength is related to surface hardness while bending fatigue strength is related to core hardness [1, 2, 3, 6, 7, 8, 9, 11, 21]. Many of the AGMA available gear nominal strength data have been developed from tests of actual gear teeth so they better represent reality than general material strength data [4]. AGMA gear material nominal strength data are determined at 99% reliability at 10^7 load cycles. Nominal strengths are usually determined experimentally in controlled environments. For field applications, the nominal strengths need adjustments, so AGMA [23] recommends several factors as modifiers.

For grade 1thru-hardened steel, the nominal contact strength may be estimated [3] as:

$$S_c^{/} = 2.15H_s + 200 \quad \text{(A1)}$$

The design strengths are obtained as:

$$S_{c1} = Y_{cs}S_{c1}^{/} \quad \text{(A2a)}$$

$$S_{c2} = Y_{cs}Y_hS_{c1}^{/} \quad \text{(A2b)}$$

$$Y_{cs} = Y_{cn}Y_{cr}Y_{cz}Y_{co} \quad \text{(A3)}$$

AGMA provides methods for evaluating most of the parameters in Eqs. (A2) and (A3). The allowable or design contact stress is:

$$S_H = \frac{\min(S_{c1},\ S_{c2})}{n_H} \quad \text{(A4)}$$

AGMA provides no specific recommendations for n_H. As a general guide, it is suggested $n_H = 1.10$ for normalized steel, $n_H = 1.20$ for quenched-tempered steel, and $n_H = 1.25$ for case-hardened steel and cast iron.